11th International Conference Interdisciplinarity in Engineering, INTER-ENG 2017, 5-6 October 2017, Tirgu-Mures, Romania

MPPT algorithms based modeling and control for photovoltaic system under variable climatic conditions

Hanane Yatimi[a],*, Elhassan Aroudam[b]

[a]Modeling and Simulation of Mechanical Systems Team, Physics Department, Faculty of Sciences,
[b]Abdelmalek Essaadi University, Sebta Ave., Mhannech II BP 2121, Tetouan, 93002, Morocco

Abstract

The output characteristic of a photovoltaic (PV) module is nonlinear and changes with solar irradiance and cell's temperature. Thus, its maximum power point (MPP) is not constant. The use of Maximum Power Point Tracking (MPPT) techniques is primordial. This paper highlights two MPPT techniques: the perturb and observe (P&O) and the sliding mode control (SMC), applied to a standalone PV system under varying climatic conditions. Simulation results show that SMC provides good performance under the climatic changes in term of stability and robustness to irradiance and temperature variations compared to P&O.

1. Introduction

To increase the efficiency of the PV system, the PV energy conversion systems must operate near the MPP, hence the need of using the Maximum power point trackers (MPPTs) which play an important role in PV power systems because they maximize the output power from a PV system for a given set of conditions and minimize

* Corresponding author.
  E-mail address: yatimi.hanane@gmail.com

the overall system cost. Different MPPT techniques have been developed and employed for tracking the MPP of PV systems such as the P&O technique [1], which is based on iterative algorithms, it is easy to implement but the oscillation problem is unavoidable, The Incremental Conductance (IC) technique [2], The fuzzy logic control search method (FLC) [3] which is used very successfully in the implementation for MPP searching, and the sliding mode control [4]. Among these existing MPPT control methods, the P&O algorithm is used in many PV systems more widely than others. The P&O method can work well when the solar irradiance and the temperature do not vary quickly with time. However, it can't track the MPP quickly and the output power is oscillating around the MPP. The paper is organized as follows. In Section 2, modeling of the overall PV system is developed. In Section 3, the two MPPT techniques P&O and SMC are carried out. In Section 4, simulation results and discussions are presented. Finally, some conclusions are drawn.

2. PV system modeling

The studied system consists of a PV module, a boost converter, A MPPT stage, and a load which is a battery.

2.1. PV module modeling

As the PV module is composed of group of cells, its model is based on that of a PV cell. Fig. 1 shows the equivalent circuit of a PV cell [4].
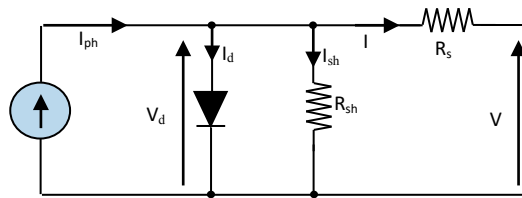

Fig. 1. Equivalent circuit of solar cell.

According to Fig. 1, the output current–voltage (I–V) characteristic of a solar photovoltaic cell is given in the following equation [4]:

$$I = I_{ph} - I_d - I_{sh} = \left[I_{SCR} + K_i \left(T - T_r \right) \right] \left(\frac{G}{1000} \right) - I_0 \left[\exp \left(\left(\frac{q}{aKT} \right) \left(V + IR_S \right) \right) - 1 \right] - \left(\frac{V + IR_S}{R_{sh}} \right) \tag{1}$$

I_{ph}: is the generated photocurrent (A), it depends mainly on the radiation and cell's temperature.
I_0: is the reverse saturation current of diode (A), it is influenced by the temperature according to Eq. 2,

$$I_0 = I_{rs} \left[\frac{T}{T_r} \right]^3 \exp \left[\left(\frac{qE_{g_s}}{aK} \right) \left(\frac{1}{T_r} - \frac{1}{T} \right) \right] \tag{2}$$

where, V is the output voltage of the PV cell (V), I is the current of the PV cell (A), I_{scr} is the short-circuit current at reference condition (A), K_i is the short-circuit temperature coefficient, T_r is the reference temperature (K), G is the solar irradiance (W/m2), I_{rs} is the saturation current at reference temperature (A), q is the electron charge ($1.60217*10^{-19}$ C), K is the Boltzmann constant ($1.38*10^{-23}$ J/K), a is the diode ideality factor, T is the temperature (K), R_s is the series resistance of the PV cell (Ω), and R_{sh} is the parallel resistance of the PV cell (Ω).

The PV module mathematical model is represented by Eq. 3. Where, N_s is the series solar cells per module, and N_p is the parallel solar cells per module.

$$I = N_p I_{ph} - N_p I_0 \left[\exp\left(\left(\frac{q}{akT} \right) \left(\frac{V}{N_s} + \frac{IR_s}{N_p} \right) \right) - 1 \right] - \frac{N_p}{R_{sh}} \left(\frac{V}{N_s} + \frac{IR_s}{N_p} \right) \tag{3}$$

2.2. Boost converter and battery model

A boost converter is a DC-to-DC converter steps up voltage. Its circuit is shown in Fig. 2.
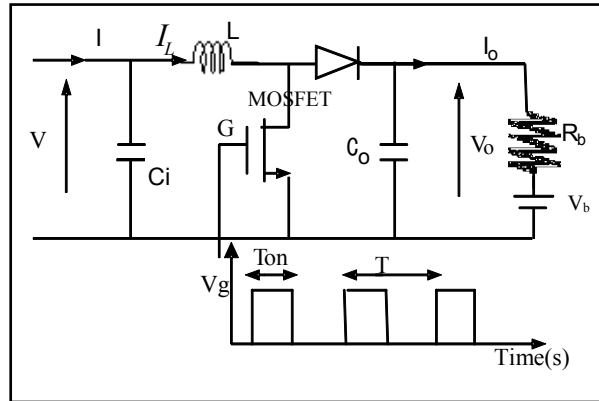

Fig. 2. Circuit of boost converter and battery.

Its duty cycle is given by: $\alpha = t_{on}/T = t_{on}/(t_{on} + t_{off})$, where T is its time period, t_{on} and t_{off} are a positive variables. The battery is considered as a constant voltage V_b in series with a constant resistance R_b. By considering the mean values of the electric quantities over a chopping period, the state equations of the converter operating in continuous conduction mode is expressed by Eq. 4. where I, V, I_L, I_o, V_o, L, C_i, C_o and α, refer to PV output current and voltage, inductor current, output current and voltage, inductance, input and output capacitor, duty cycle of the boost converter, respectively.

$$C_i \frac{dV}{dt} = I - I_L; \quad L \frac{dI_L}{dt} = V - (1-\alpha)(V_b + R_b I_o); \quad C_o R_b \frac{dI_o}{dt} = -I_o + (1-\alpha)I_L \tag{4}$$

2.3. System model

By combining the equations Eq. 3 and Eq. 4 describing the system, the nonlinear mathematical model of the PV storage system can be expressed in state space by Eq. 5 with:

$$x_1 = V; \quad x_2 = I_L; \quad x_3 = V_o; \quad u = 1 - \alpha; \quad y = \frac{\partial P}{\partial V}$$

$$\begin{cases} \dot{x}_1 = \dfrac{I}{C_i} - \dfrac{1}{C_i} x_2 \\[2mm] \dot{x}_2 = \dfrac{1}{L} x_1 - \dfrac{\mu}{L} x_3 \\[2mm] \dot{x}_3 = \dfrac{V_b}{C_o R_b} + \dfrac{1}{C_o R_b} x_3 + \dfrac{\mu}{C_o} x_2 \end{cases} \tag{5}$$

Based on the power-voltage characteristic curves of the PV module, when the PV module is operating in its maximum power point $P=V.I$, we can get:

$$\frac{\partial P}{\partial V} = \frac{\partial (V.I)}{\partial V} = I + V \frac{\partial I}{\partial V} = 0 \tag{6}$$

The output system to be forced to zero in finite time is: $y=dP/dV$. The relative degree $r = 2$ of the system corresponds to the number of times the output y has to be differentiated with respect to time before the input u appears explicitly in the resulting equations. We have the first and second time derivative of the controlled output y, after the second derivation of the output of the system we obtain the expression represented by Eq.7. u is considered as the applied control law and α can be deducted from $u = 1 - α$ with the main objective of u is to steer the output to zero in finite time.

$$\ddot{y} = f(x,t) + g(x,t)u \tag{7}$$

$$f(x,t) = \left(\frac{\partial^3 P}{\partial v^3} \right) \left(\frac{\partial V}{\partial t} \right)^2 + \frac{1}{C_i} \left(\frac{\partial^2 P}{\partial V^2} \right) \left[\left(\frac{\partial I}{\partial V} \right) \left(\frac{\partial V}{\partial t} \right) - \frac{V}{L} \right] \tag{8}$$

$$g(x,t) = \frac{1}{C_i} \left(\frac{\partial^2 P}{\partial V^2} \right) \frac{V_o}{L} \tag{9}$$

3. MPPT technique for PV system

3.1. Perturbation and observation technique (P&O)

The application of the P&O algorithm has been widely employed in practice due to its simplicity and ease of implementation [5]. The P&O techniques operate by periodically perturbing (i.e. incrementing or the module terminal voltage and comparing the PV output power with that of the previous perturbation cycle. If the PV module operating voltage changes and power increases, the control system moves the PV module operating point in that direction; otherwise the operating point is moved in the opposite direction. The major disadvantages of the P&O technique are occasional deviation from the maximum operating point in case of rapidly changing atmospheric conditions, such as broken clouds [5].

3.2. Sliding Mode Control (SMC)

The basic principle of the SMC consists in moving the state trajectory of the system toward a predetermined surface called sliding or switching surface [6] and in maintaining it around this latter with an appropriate switching logic. The design of SMC involves two tasks. The first one involves the design of a sliding surface S where the switching function σ =0, so that the sliding motion satisfies the design specifications. The second one is to design the discontinuous control such that the system enters the sliding mode σ and remains in it forever [7]. These conditions are obtained from geometrical considerations: the deviation from the switching function σ and its time derivative $\dot{\sigma}$ should be opposite signs in the vicinity of a sliding surface. These conditions are usually written more conveniently as $\sigma\dot{\sigma}<0$.

The sliding surface is chosen according to the output to be forced to zero in finite time and the relative degree of the system. The relative degree of the system r is defined to be the least positive integer i for which the derivative $y^{(i)}(t)$ is an explicit function of the control law $u(t)$ such that:

$$\frac{\partial y^{(r)}(t)}{\partial u} \neq 0 \quad \text{and} \quad \frac{\partial y^{(i)}(t)}{\partial u} = 0 \quad \text{for } i = 0, \dots, r-1.$$

The switching function can be selected as follows:

$$\sigma(t) = y^{(r-1)}(t) + \lambda_{r-2} \, y^{(r-2)}(t) + \dots + \lambda_0 \, y(t)$$

where the coefficients $\lambda_0 \dots \lambda_{r-2}$ are chosen so that the characteristic polynomial associated to $\sigma(t)$ have its roots strictly in the left half complex plane. Then, the output $y(t)$ tends asymptotically to zero in a finite time when σ tends to zero in a finite time. In sliding surface, $\sigma(t) = 0$. In our application $r = 2$ and the switching function:

$$\sigma = \lambda y + \dot{y} \quad \Rightarrow \quad \dot{\sigma} = \lambda \dot{y} + \ddot{y} \tag{10}$$

where λ is a positive constant. Replacing $\ddot{y}$ by its expression (7), we obtain:

$$\dot{\sigma} = F + g\, u \tag{11}$$

The control law $u(t)$ forcing approximately the output y to zero in finite time is composed of two terms u_{eq} and u_r as follow:

$$u = u_{eq} + u_r \tag{12}$$

where u_{eq} is the equivalent linear control term which makes the undisturbed nominal system state slide on the sliding surface, and u_r is the term forcing the system to remain on the sliding surface in presence of disturbances and parameters variations. To determine these two terms, two state of the sliding surface will be considered.
In sliding surface where σ(t)=0, $u=u_{eq}$ is the control law obtained from the equivalent control method which is determined from the solution of equation $\dot{\sigma}(t) = 0$ in (11), we obtain:

$$u = u_{eq} = -F\big/g \tag{13}$$

For the disturbed switching function $\sigma(t) \neq 0$, in order to demonstrate stability, the candidate Lyapunov function is adopted:

$$V = 1\big/2\, \sigma(t)^2 \tag{14}$$

Then:

$$\dot{V} = \sigma \dot{\sigma} \tag{15}$$

By choosing:

$$\dot{\sigma} = -k\, sign(\sigma) \tag{16}$$

$$\dot{V} = -k\, \sigma\, sign(\sigma) = -k\, |\sigma| < 0 \tag{17}$$

where k is a positive parameter. From (11) and (16), we have:

$$u = u_{eq} + u_r = -F/g - k/g \, sign(\sigma) \tag{18}$$

4. Simulation results and discussions

Simulation results are given with Matlab/Simulink to validate the proposed control strategy in rapid temperature and solar irradiance changes. The Mono-crystalline SW 255 Mono PV module has been chosen to validate the model. The used PV storage system has the parameters summarizes in the table 1.

Table 1. Simulation parameters.

Parameter	Name	Value
PV module SW 255 Mono		
P_{max}	Maximum Power	255 W
V_{mpp}	Voltage at Maximum Power	30.6 V
I_{mpp}	Current at Maximum Power	8.43 A
V_{oc}	Open Circuit Voltage	38.7 V
I_{sc}	Short Circuit Current	9.05 A
R_s	Series resistance	0.3058 Ω
R_{sh}	Parallel resistance	50 kΩ
a	Ideality factor	1.3352
I_{SCR}	Short circuit current at STC	9.0501 A
I_{rs}	saturation current at T_r	$6.2217.10^{-8}$ A
K_i	Temperature coefficient	$4.4.10^{-4}$ A/K
T_r	Reference temperature	298.15 K
DC-DC converter		
L	Inductance	2.2 mH
C_i	Input capacitor	47 mF
C_o	Output capacitor	4.7 mF
Battery		
V_b	Battery voltage	48 V
R_b	Battery resistance	2 Ω

4.1. Theoretical results

For different values of solar irradiance *G* and temperature *T*, the computation of the theoretical optimum values of duty cycle *α*, PV voltage *V*, PV current *I*, PV power *P* is assembled in table 2.

Table 2. Theoretical results for given solar irradiance and temperature.

Values of G (W/m²) /T (K)	I(A)	V (V)	P(W)	α
800/ 298.15 (25°C)	6.7526	30.6350	206.8647	0.4476
1000/298.15 (25°C)	8.4301	30.6178	258.1111	0.4633
1000/308.15 (35°C)	8.3890	29.4301	246.8896	0.4810

4.2. Simulation results and analysis

A simulation study was made to illustrate the response of the system to solar irradiance *G* and module temperature *T* variation. For this purpose, the irradiance *G* and module temperature *T*, which are initially at 800 *W/m²* and 298.15 *K (25°C)*, are respectively switched at 3 s and 6 s to 1000 *W/m²* and *308.15K* (35°C).

Figs. 3-6 show respectively the good concordance between the PV current, the PV voltage, the PV power of the PV module and the duty cycle control of the boost converter with the theoretical results, with the problem of the oscillations around the MPP, which causes the PV energy losses for P&O technique, and without oscillations for SMC technique.

Fig. 7 shows the evolution of the controlled output *y* and the sliding surface. When the maximum power is reached, the sliding surface and the controlled output *y=dP/dv* converge to zero. This way, the robustness of the system control to solar irradiance and temperature changes is evaluated.

It is concluded from the simulations that, when the solar irradiance and temperature varies, the duty cycle of the boost converter α is judiciously adjusted to its desired value (Fig. 6), which forces the PV module voltage to follow its optimal value (Fig. 4). Consequently, the PV module power reached its maximal value (Fig. 5).
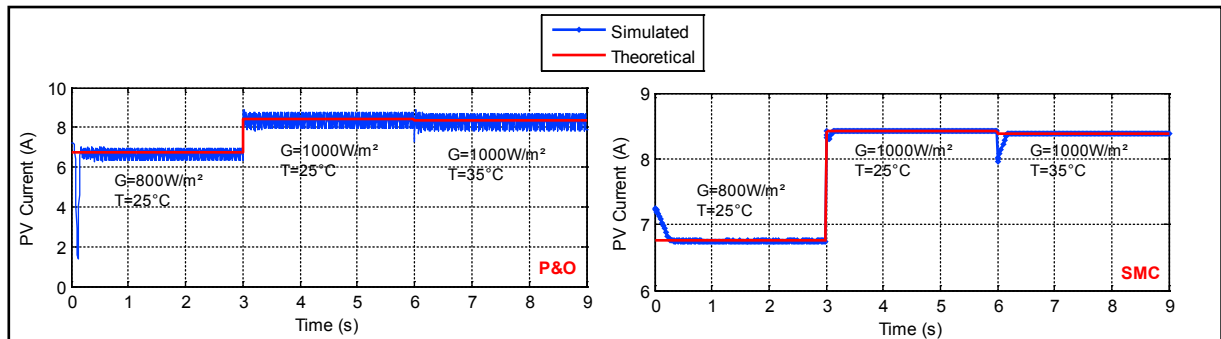

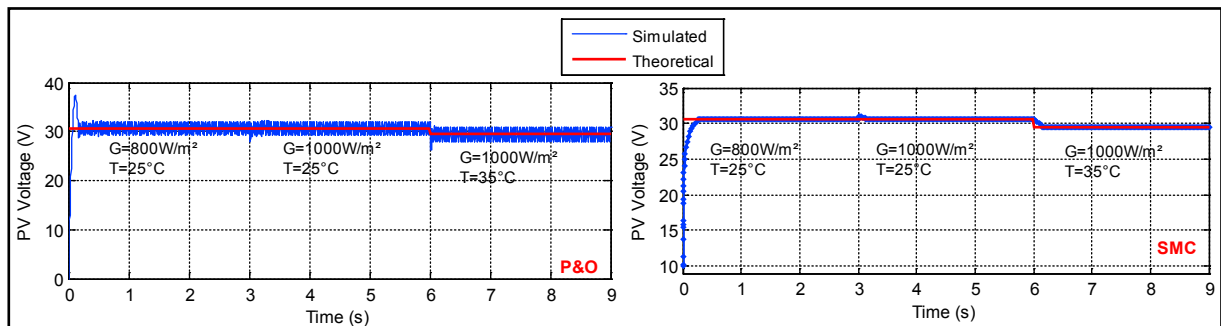Fig. 3. PV current variation.

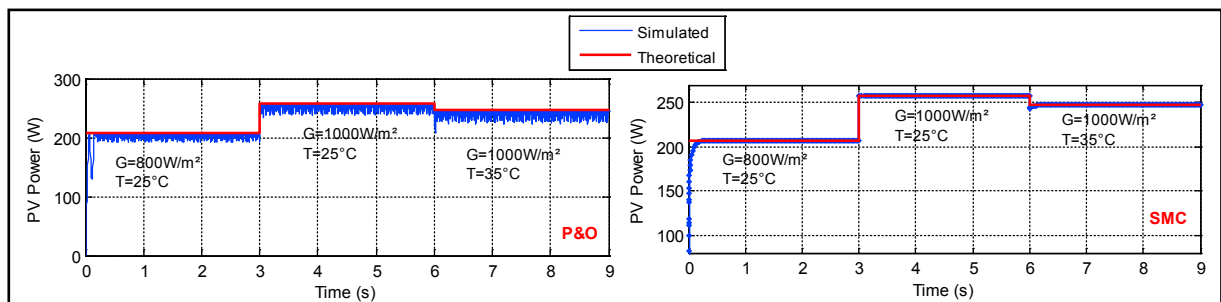

Fig. 4. PV voltage variation.
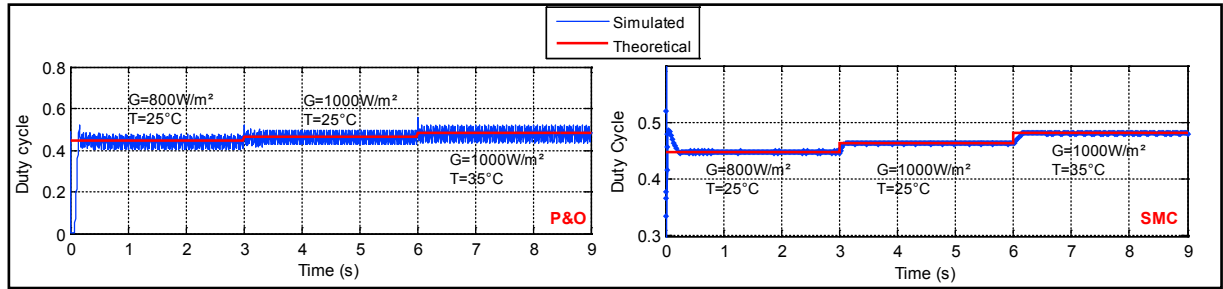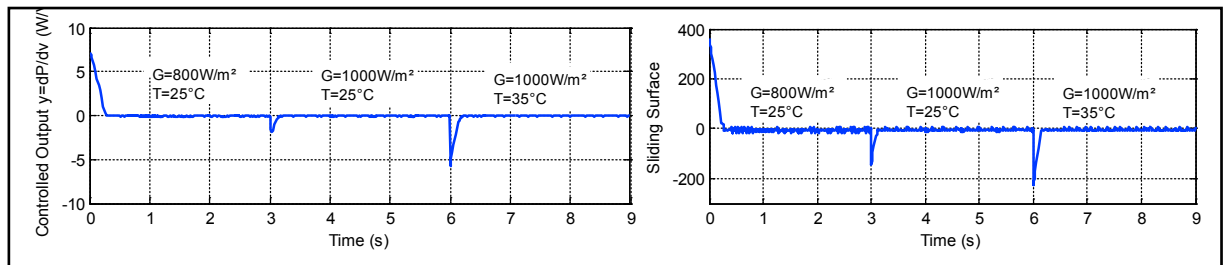

Fig. 5. PV power variation.

Fig. 6. Duty cycle variation.

Fig. 7. Controlled output (y=dP/dV) and Sliding surface.

5. Conclusion

This paper provides two MPPT techniques, the P&O and the SMC techniques, applied to a stand-alone PV system with battery storage. The proposed system was simulated in Matlab/Simulink software. Simulation results show that the P&O technique is simple, but has considerable power loss because PV module can only run in oscillation way around the MPP. Whereas, the SMC technique has shown better performance. It ensures better tracking performance and high robustness, regardless of the ranges of variation of meteorological parameters; the responses are more stable, more accurate and robust.

References

[1] N. Femia, et al, Optimization of perturb and observe maximum power point tracking method. IEEE Trans Power Electron. 20 (4) (2005) 963–73.

[2] A. Zegaoui, M. Aillerie, P. Petit, J.P. Sawicki, A. Jaafar, C. Salame, J.P. Charles, Comparison of two common maximum power point trackers by simulating of PV generators. Energy Proceedia, 6 (2011) 678–687.

[3] A. Messai, A. Mellit, A. Guessoum, S.A. Kalogirou, Maximum power point tracking using a GA optimized fuzzy logic controller and its FPGA implementation. Solar Energy. 85 (2011) 265–277.

[4] H. Yatimi, E. Aroudam, Assessment and control of a photovoltaic energy storage system based on the robust sliding mode MPPT controller. Solar Energy. 139 (2016) 557–568.

[5] B. Bendib, H. Belmili, F. Krim, A survey of the most used MPPT methods: Conventional and advanced algorithms applied for photovoltaic systems. Renewable and Sustainable Energy Reviews. 45 (2015) 637–648.

[6] J. Soltani, A.F. Payam, A robust adaptive sliding-mode controller for slip power recovery induction machine drives. Power Electronics and Motion Control Conference vol. 3, 2006, pp. 1-6.

[7] Y. Levron, D. Shmilovitz, Maximum Power Point Tracking Employing Sliding Mode Control, IEEE Transactions on Circuits and Systems. 60(3) (2013) 724-732.